Atomically resolved $Au_{52}Cu_{72}(SR)_{55}$ nanoalloy reveals Marks decahedron truncation and Penrose tiling surface

Song *et al*

Supplementary Table 1 Crystal data and structure refinement for $[Au_{52}Cu_{72}(p\text{-MBT})_{55}]^{+}Cl^{-}$.

Identification code	$Cu_{72}Au_{52}$
Empirical formula	$C_{385}H_{385}Au_{52}ClCu_{72}S_{55}$
Formula weight	21627.80
Temperature/K	123
Crystal system	triclinic
Space group	$P\bar{1}$
a/Å	25.8880(19)
b/Å	26.7997(18)
c/Å	45.013(3)
α/°	79.828(2)
β/°	85.255(3)
γ/°	69.166(2)
Volume/Å^3	28722(3)
Z	2
ρ_{calc}g/cm^3	2.501
μ/mm^{-1}	32.176
F(000)	19576.0
Crystal size/mm^3	0.42 × 0.22 × 0.20
Radiation	GaK_α (λ = 1.34139)
2Θ range for data collection/°	1.736 to 110.384
Index ranges	$-31 \le h \le 31$, $-32 \le k \le 32$, $-40 \le l \le 54$
Reflections collected	356930
Independent reflections	108535 [R_{int} = 0.0445, R_{sigma} = 0.0475]
Data/restraints/parameters	108535/0/5042
Goodness-of-fit on F^2	1.090
Final R indexes [I>=2σ (I)]	R_1 = 0.0388, wR_2 = 0.1090
Final R indexes [all data]	R_1 = 0.0525, wR_2 = 0.1146
Largest diff. peak/hole / e Å^{-3}	3.92/-2.15

Supplementary Table 2 The result of ICP-MS analysis on the $[Cu_{72}Au_{52}(p\text{-MBT})_{55}]^+$ nanoalloy.

	Cu (ppm)	Au (ppm)	Cu : Au (mol)
$Cu_{72}Au_{52}$	91.38	204.34	72 : 51.89
	40.43	90.46	72 : 51.92
	105.69	237.21	72 : 52.08

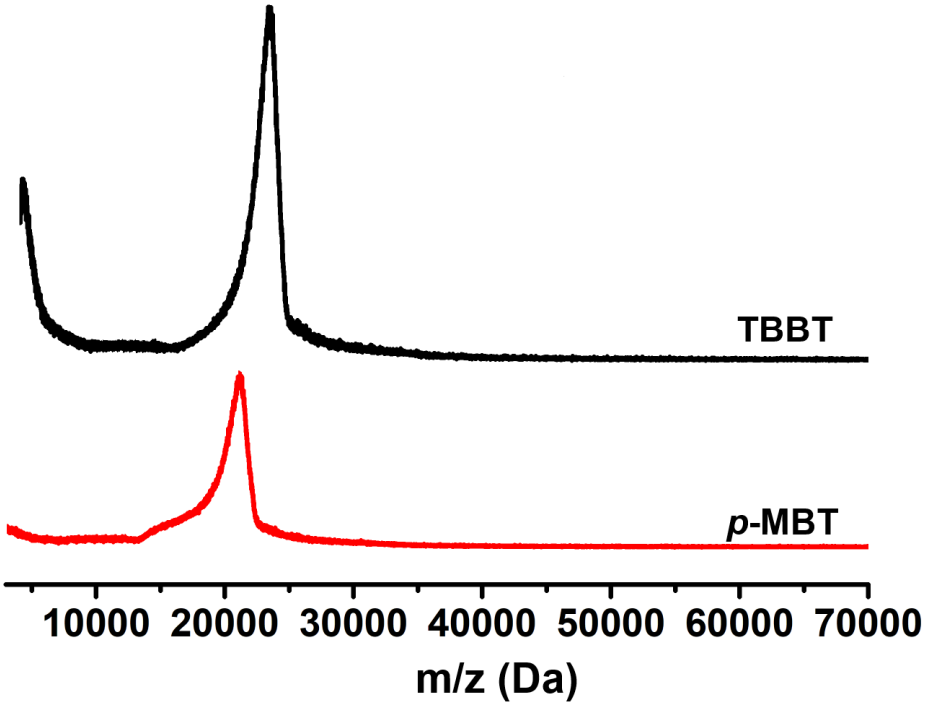

Supplementary Fig 1 MALDI mass spectra of $[Au_{52}Cu_{72}(SR)_{55}]^+$ capped by *p*-MBT (red) or TBBT (black) in positive mode (TBBT = SPh-^{t}Bu and *p*-MBT = SPh-*p*-CH_3).

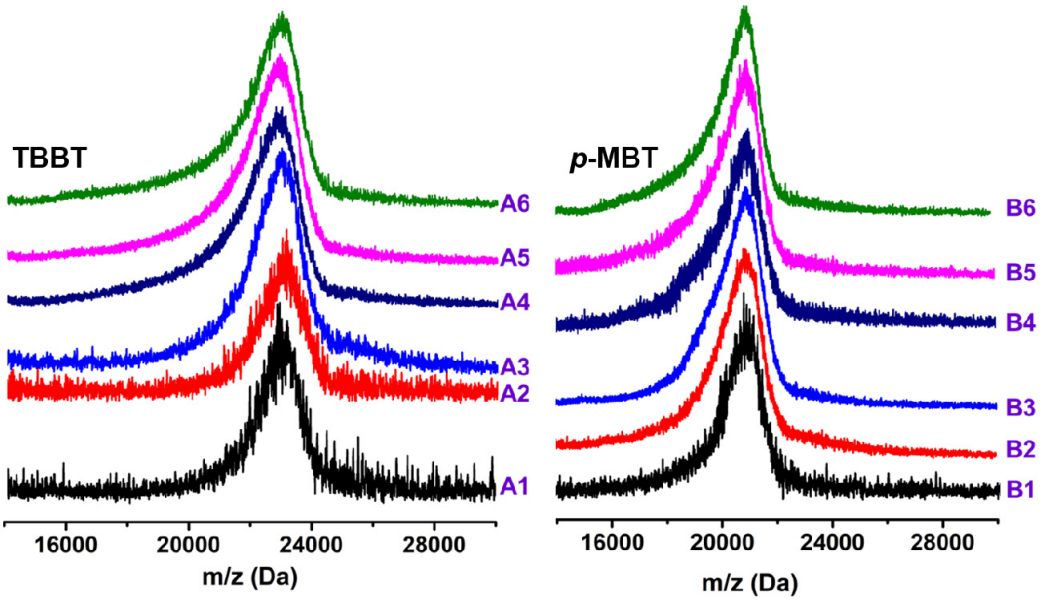

Supplementary Fig 2 Intensity-dependent MALDI mass spectra of $[Au_{52}Cu_{72}(TBBT)_{55}]^+$ (left panel) and $[Au_{52}Cu_{72}(p\text{-MBT})_{55}]^+$ (right panel) nanoalloys. The different parameters (A1/B1-A5/B5) in MALDI-MS are listed in Table S3.

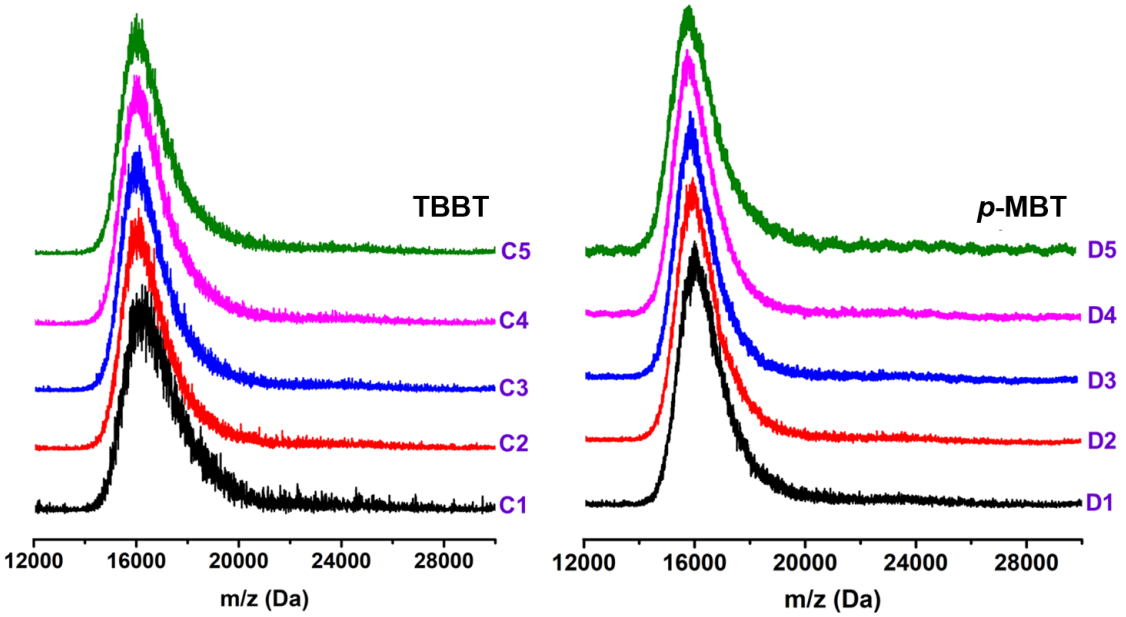

Supplementary Fig 3 Intensity-dependent LDI mass spectra of $[Au_{52}Cu_{72}(TBBT)_{55}]^+$ (left) and $[Au_{52}Cu_{72}(p\text{-MBT})_{55}]^+$ (right) nanoalloys. The different parameters (C1/D1-C5/D5) in LDI-MS are listed in Table S3.

Supplementary Table 3 Different parameters in MALDI/LDI-MS

	A1/B1	A2/B2	A3/B3	A4/B4	A5/B5	A6/B6	C1/D1	C2/D2	C3/D3	C4/D4	C5/D5
Offset	55%	60%	70%	80%	90%	70%	60%	70%	80%	90%	70%
Range	20%	20%	20%	20%	10%	30%	20%	20%	20%	10%	30%
Linear	90X	90X	90X	90X	90X	90X	90X	90X	90X	90X	90X
Percent	100%	100%	100%	100%	100%	100%	100%	100%	100%	100%	100%

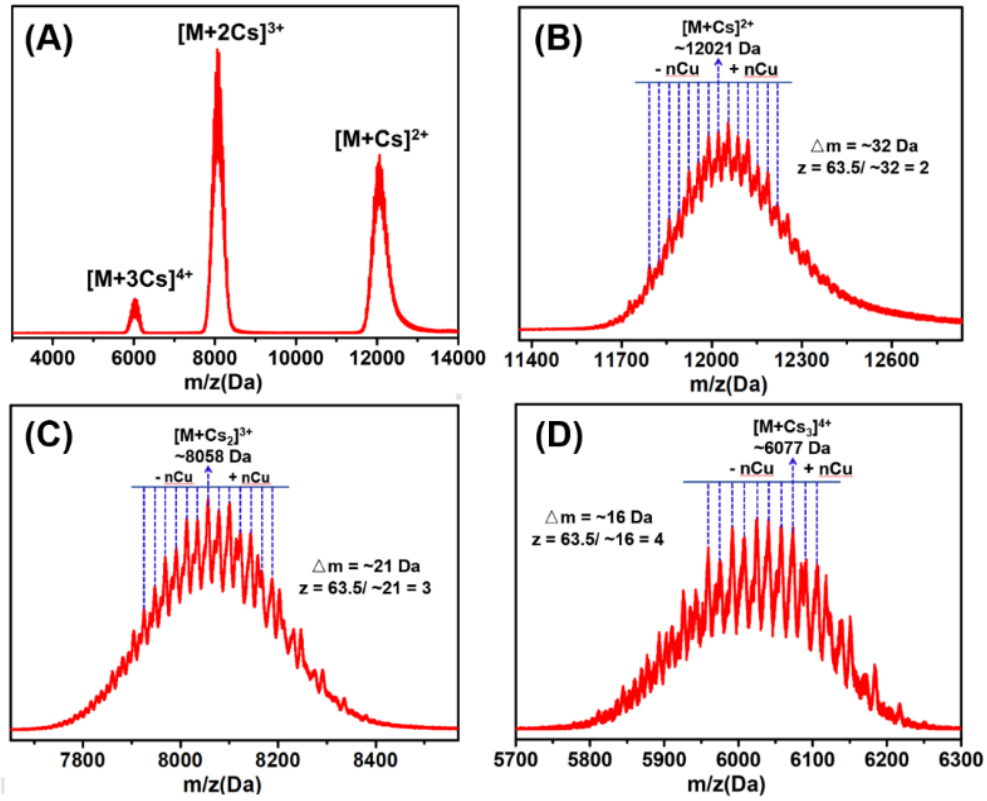

Supplementary Fig 4 The ESI mass spectrum of the $[Au_{52}Cu_{72}(TBBT)_{55}]^+$ in positive mode by adding Cs^+. (A) Full spectrum, (B) Zoom-in of the 2+ ion set, (C) Zoom-in of the 3+ ion set, and (D) Zoom-in of the 4+ ion set.

Supplementary Table 4 The assignments of the peaks in each set in the ESI mass spectrum.

Peaks in set a		**Peaks in set b**		**Peaks in set c**	
value	Assigned formula	value	Assigned formula	value	Assigned formula
12178	$[Au_{52}Cu_{77}(SR)_{55}Cs]^{2+}$	8163	$[Au_{52}Cu_{77}(SR)_{55}Cs_2]^{3+}$	6156	$[Au_{52}Cu_{77}(SR)_{55}Cs_3]^{4+}$
12147	$[Au_{52}Cu_{76}(SR)_{55}Cs]^{2+}$	8142	$[Au_{52}Cu_{76}(SR)_{55}Cs_2]^{3+}$	6140	$[Au_{52}Cu_{76}(SR)_{55}Cs_3]^{4+}$
12115	$[Au_{52}Cu_{75}(SR)_{55}Cs]^{2+}$	8121	$[Au_{52}Cu_{75}(SR)_{55}Cs_2]^{3+}$	6124	$[Au_{52}Cu_{75}(SR)_{55}Cs_3]^{4+}$
12083	$[Au_{52}Cu_{74}(SR)_{55}Cs]^{2+}$	8099	$[Au_{52}Cu_{74}(SR)_{55}Cs_2]^{3+}$	6108	$[Au_{52}Cu_{74}(SR)_{55}Cs_3]^{4+}$
12052	$[Au_{52}Cu_{73}(SR)_{55}Cs]^{2+}$	8078	$[Au_{52}Cu_{73}(SR)_{55}Cs_2]^{3+}$	6092	$[Au_{52}Cu_{73}(SR)_{55}Cs_3]^{4+}$
12021	**$[Au_{52}Cu_{72}(SR)_{55}Cs]^{2+}$**	**8058**	**$[Au_{52}Cu_{72}(SR)_{55}Cs_2]^{3+}$**	**6077**	**$[Au_{52}Cu_{72}(SR)_{55}Cs_3]^{4+}$**
11988	$[Au_{52}Cu_{71}(SR)_{55}Cs]^{2++}$	8036	$[Au_{52}Cu_{71}(SR)_{55}Cs_2]^{3+}$	6060	$[Au_{52}Cu_{71}(SR)_{55}Cs_3]^{4+}$
11956	$[Au_{52}Cu_{70}(SR)_{55}Cs]^{2+}$	8015	$[Au_{52}Cu_{70}(SR)_{55}Cs_2]^{3+}$	6044	$[Au_{52}Cu_{70}(SR)_{55}Cs_3]^{4+}$
11924	$[Au_{52}Cu_{69}(SR)_{55}Cs]^{2+}$	7994	$[Au_{52}Cu_{69}(SR)_{55}Cs_2]^{3+}$	6029	$[Au_{52}Cu_{69}(SR)_{55}Cs_3]^{4+}$
11893	$[Au_{52}Cu_{68}(SR)_{55}Cs]^{2+}$	7973	$[Au_{52}Cu_{68}(SR)_{55}Cs_2]^{3+}$	6013	$[Au_{52}Cu_{68}(SR)_{55}Cs_3]^{4+}$
11861	$[Au_{52}Cu_{67}(SR)_{55}Cs]^{2+}$	7951	$[Au_{52}Cu_{67}(SR)_{55}Cs_2]^{3+}$	5997	$[Au_{52}Cu_{67}(SR)_{55}Cs_3]^{4+}$

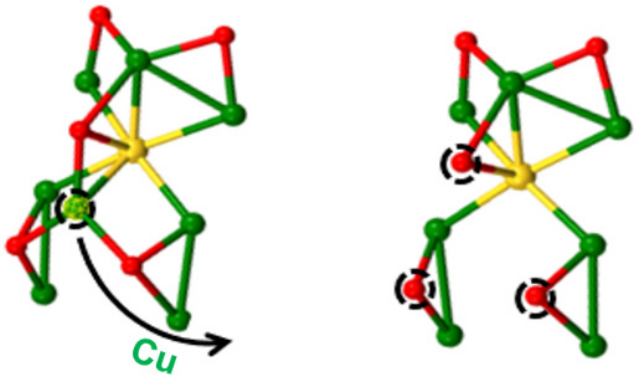

Supplementary Fig 5 A possible pathway for losing surface Cu atoms under ESI-MS conditions (Cu: green, S: red).

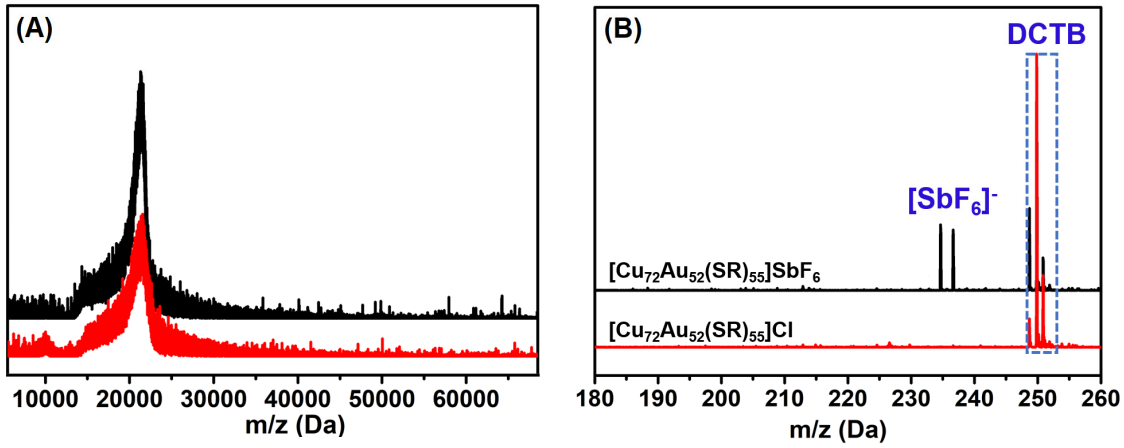

Supplementary Fig 6 Experimental proof for the existence of Cl^- in the $[Cu_{72}Au_{52}(p\text{-MBT})_{55}]Cl$ nanoalloys. (A) High-mass range spectra of $[Au_{52}Cu_{72}(p\text{-MBT})_{55}]Cl$ (red spectrum) and $[Au_{52}Cu_{72}(p\text{-MBT})_{55}]SbF_6$ (black); (B) low-mass range spectra, in which the peaks for $[SbF_6]^-$ were found in addition to those from the matrix (i.e., DCTB (*trans*-2-[3-(4-*tert*-Butylphenyl)-2-methyl-2-propenylidene]malononitrile)).

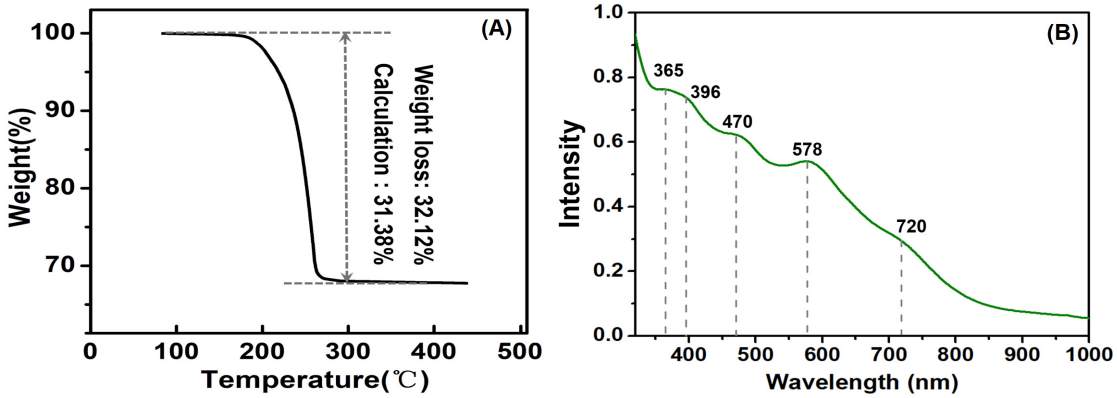

Supplementary Fig 7 (A) The thermogravimetric analysis, and (B) The UV-vis absorption spectrum of $[Cu_{72}Au_{52}(p\text{-MBT})_{55}]^+$ nanoalloys.

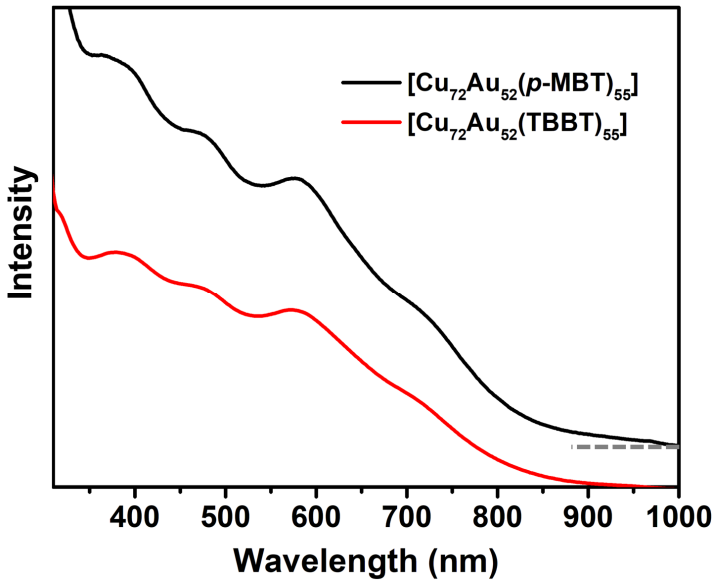

Supplementary Fig 8 UV-vis absorption spectra of two $[Cu_{72}Au_{52}(SR)_{55}]^+$ nanoalloys protecting by different ligands.

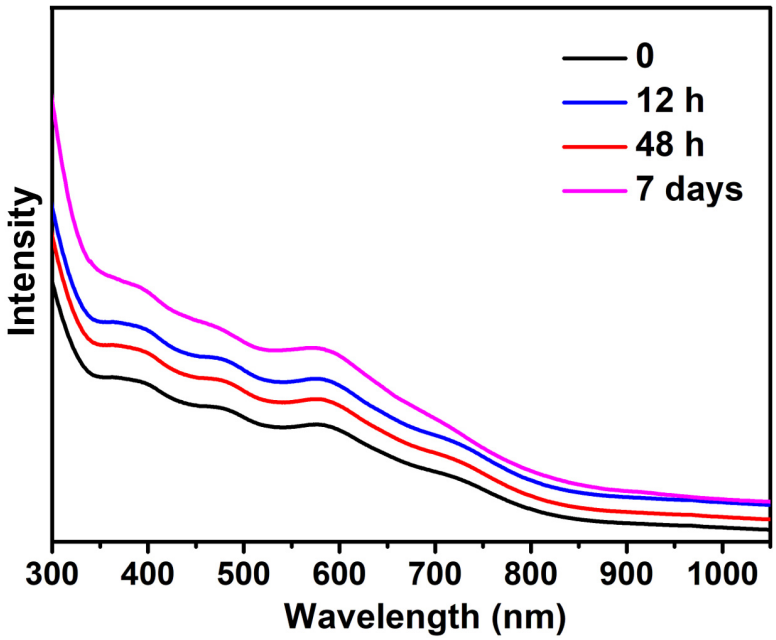

Supplementary Fig 9 Time-dependent UV-vis absorption spectra of $[Cu_{72}Au_{52}(SR)_{55}]^+$ nanoalloys in CH_2Cl_2 in the air atmosphere (room temperature).

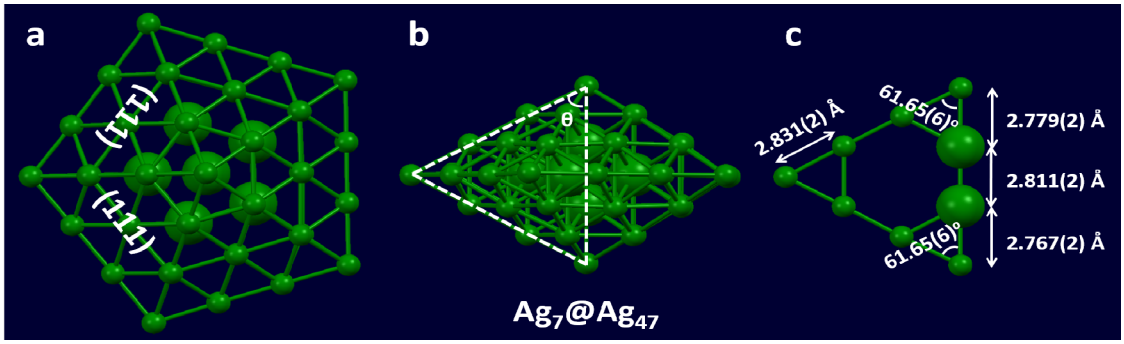

Supplementary Fig 10 (a) top view and (b) side view of the $Ag_7@Ag_{47}$ shells in Ag_{136} (ref. 30) and (c) the triangle formed by twinning edges and apex in the Ag_{47} shell.

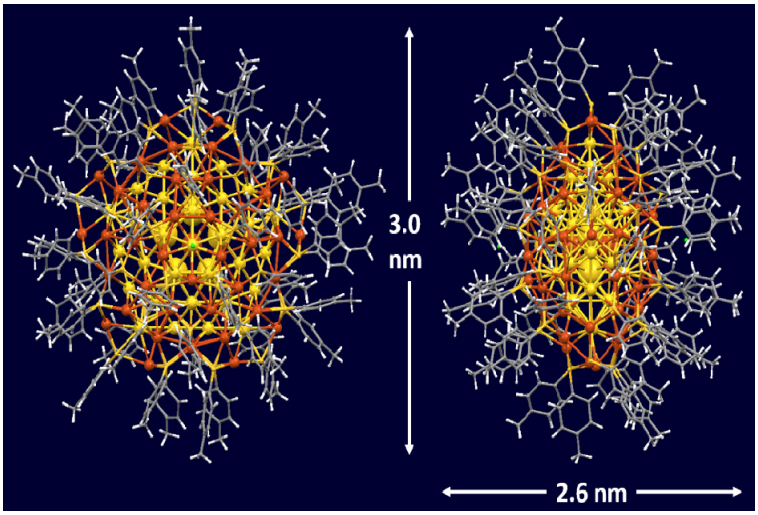

Supplementary Fig 11 The overall size of $[Cu_{72}Au_{52}(SR)_{55}]^+$.

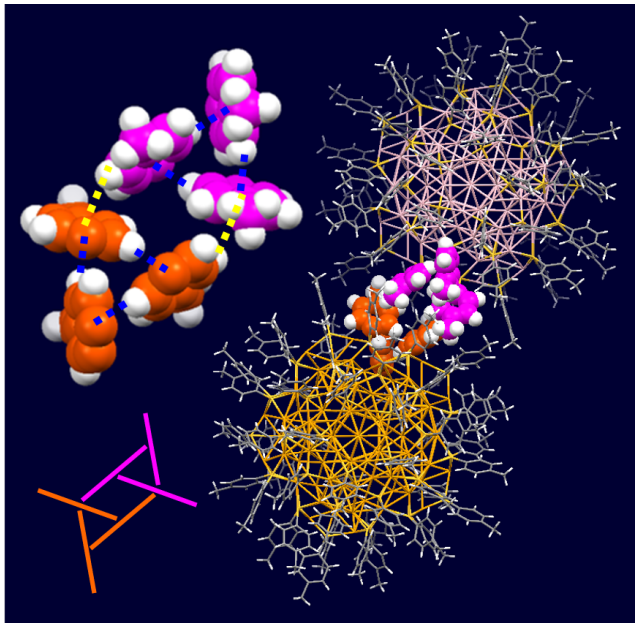

Supplementary Fig 12 Intra- and inter-cluster interactions between two $[Cu_{72}Au_{52}(SR)_{55}]^+$ nanoalloy in an edge-to-edge approach, showing six interacting *p*-MBT ligands in a triangular mosaic pattern. Color labels: pink, light orange = Au/Cu, yellow = S, grey, magenta, orange = C, and white = H.

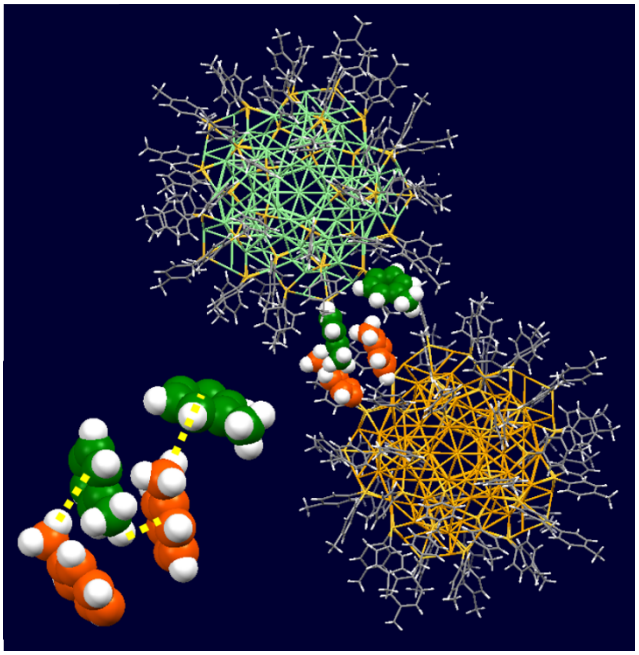

Supplementary Fig 13 Inter-cluster interactions between two $[Cu_{72}Au_{52}(SR)_{55}]^+$ nanoalloys in a tip-to-tip approach. Color labels: light green, light orange = Au/Cu, yellow = S, grey, green, orange = C, and white = H.

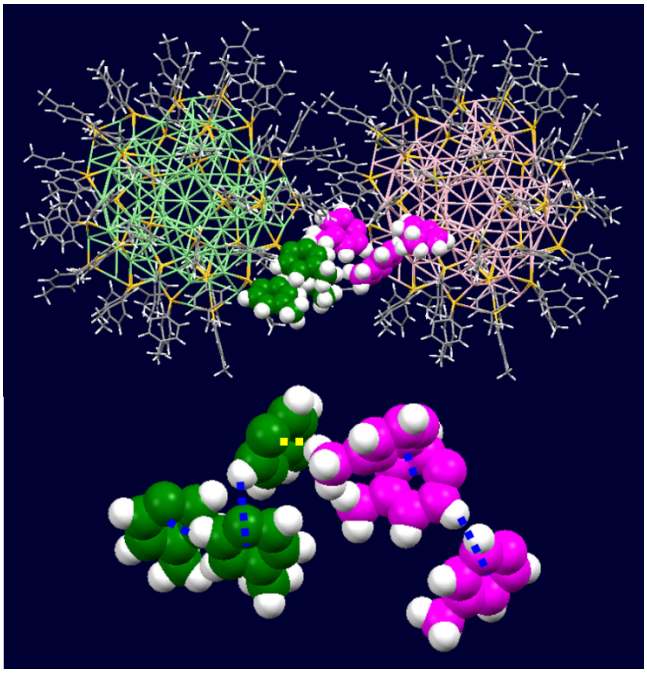

Supplementary Fig 14 Intra- and inter-cluster interactions between two $[Cu_{72}Au_{52}(SR)_{55}]^+$ nanoalloy in a tip-to-edge approach. Color labels: light green, pink = Au/Cu, yellow = S, grey, green, magenta = C, and white = H.

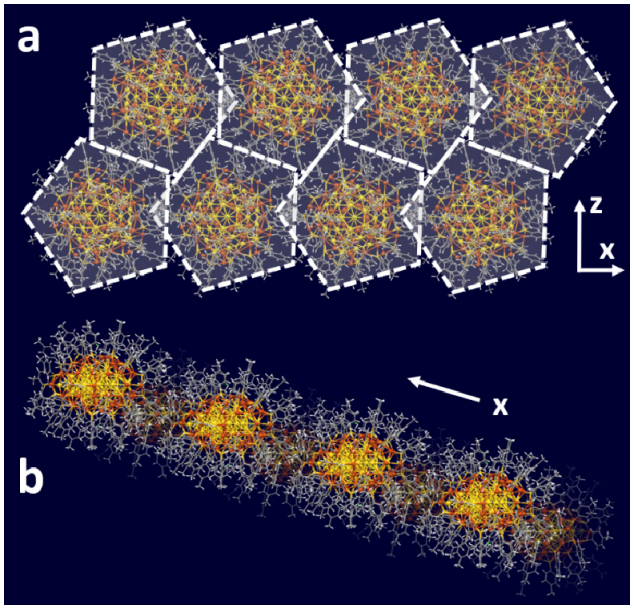

Supplementary Fig 15 (a) front and (b) top view of the twin nanowire formed by interlocked $[Cu_{72}Au_{52}(SR)_{55}]^+$ nanoalloys along x axis.

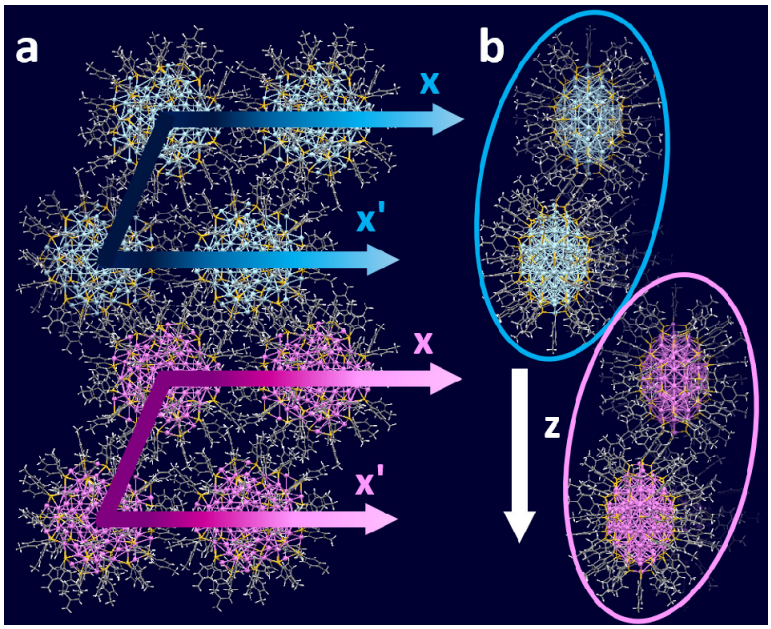

Supplementary Fig 16 (a) front and (b) side view of the two sets of nanowires which are not interact along z axis. Each nanowire is composed of two lines (x and x') of interlocked $[Cu_{72}Au_{52}(SR)_{55}]^{+}$ nanoalloys.

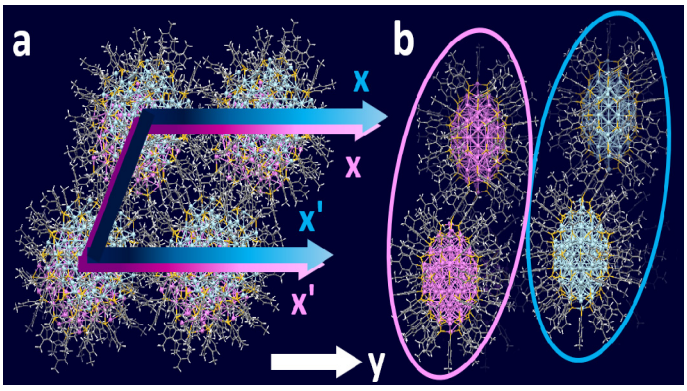

Supplementary Fig 17 (a) front and (b) top view of the two sets of nanowires which are not interact along y axis. Each nanowire is composed of two lines (x and x') of interlocked $[Cu_{72}Au_{52}(SR)_{55}]^{+}$ nanoalloys.